Lipidomics Analysis Reveals Protective Effect of Myriocin on Cerebral Ischemia/Reperfusion Model Rats

Ting Wang (867176431@qq.com)
The First Affiliated Hospital of ZhenZhou University https://orcid.org/0000-0002-8847-0036
Jingmin Zhang
The First Affiliated Hospital of ZhenZhou University
Meng Yang
The First Affiliated Hospital of ZhenZhou University
Jinxiu Guo
The First AFFiliated Hospital of ZhenZhou University
Duolu Li
The First Affiliated Hospital of ZhenZhou University https://orcid.org/0000-0001-8410-359X
Ying Li
The First Affiliated Hospital of ZhenZhou University

Research Article

Keywords: Myriocin, Cerebral ischemia/reperfusion injury, Lipidomics, UPLC-Q-TOF/MS

Posted Date: February 15th, 2022

DOI: https://doi.org/10.21203/rs.3.rs-1324750/v1

Abstract

Ceramide accumulation has been associated with ischemic stroke. Myriocin is an effective SPT inhibitor, which reduces the levels of ceramides by inhibiting *de novo* synthesis pathway. However, the role of myriocin in cerebral ischemia/reperfusion (I/R) injury and its underlying mechanism remains unknown. The present study established an experimental rat model of middle cerebral artery occlusion (MCAO). We employed UPLC-Q-TOF/MS-based lipidomic analysis to identify the disordered lipid metabolites and the effects of myriocin in cerebral cortical tissues of rats. In this study, we found 15 characterized lipid metabolites involved in sphingolipid and glycerophospholipid metabolism in cerebral I/R-injured rats, which were significantly reversed by myriocin. Specifically, the mRNA expression of metabolism-related enzyme genes was detected by real-time quantitative polymerase chain reaction (RT-qPCR).We demonstrated that myriocin could regulate the mRNA expression of ASMase, NSMase, SGMS1, SGMS2, ASAH1, ACER2, ACER3 involved in sphingolipid metabolism and PLA2 involved in glycerophospholipid metabolism. Moreover, TUNEL and western blot assay showed that myriocin played a key role in regulating neuronal cell apoptosis. In summary, the present work provides a new perspective for a systematic study of metabolic changes in ischemia stroke and the therapeutic applications of myriocin.

Introduction

Cerebral ischemia/reperfusion (I/R) injury is caused by blood supply restriction and followed by the restoration of blood flow and re-oxygenation (Peralta, 2013), and it typically occurs during the treatment stage of ischemic disease, aggravating irreversible brain tissue harm (Obadia, 2017; Yu, 2018). Numerous studies have confirmed that ischemic/reperfusion of the brain leads to a cascade of pathological mechanisms, mainly involving neuronal excitotoxicity, oxidative stress, ionic imbalance and so on (Khandelwal, 2016; Lai, 2014; Schaller, 2003). In clinical practice, reperfusion treatments based on thrombolysis and mechanical thrombectomy are major therapeutic strategies for ischemic stroke patients. The risk of cerebral ischemia/reperfusion injury following reperfusion therapy is a critical challenge for patient outcomes(Cas, 2020). Moreover, in view of the clinical therapeutic limitations of ischemic stroke, it is urgently required to develop efficient therapeutic strategies and potential drugs to treat ischemic stroke.

Lipids are essential components of cellular membranes and play a vital role in cell development and death(Wu, 2018). Compared to other organs in mammalians, the brain not only contains extremely abundant lipids, but a large diversity of lipid species is identified(Fitzner, 2020). Notably, growing evidence has indicated lipid metabolism disorders were tightly associated with the occurrence of disease(Doria, 2011; Naudí, 2015; Orei et al., 2012). Ceramides, a bioactive sphingolipid, is a critical class of signalling molecule that acts as a second messenger in a sphingolipid signal transduction(Fyrst, 2010). Previous studies have shown that ceramide accumulation was observed after ischemic injury, which supported a distinctly link between ceramide and ischemic stroke(Bhuiyan, 2010; Novgorodov, 2015; Yu, 2007).

Myriocin is a powerful inhibitor of the serine palmitoyltransferase (SPT), which catalyzes the first step of ceramide synthesis(Wadsworth, 2013). Furthermore, Myriocin (Fig. 1) is a new small molecule immunosuppressant extracted from *Mycelia sterilia, Isaria sinclairii* and *Cordyceps cicadae*(Wadsworth, 2013). In particular, myriocin has been extensively utilized for studying certain diseases related to sphingolipids(Cheng, 2016; Lee, 2011). Other studies have demonstrated that myriocin treatment was proposed as a strategy for myocardial ischemia/reperfusion injury(Bonezzi et al., 2019; Reforgiato et al., 2016). However, the underlying protection mechanism exerted by myriocin against ischemic stroke is yet to be reported.

Lipidomics presents a comprehensive analysis of lipid metabolic profiles in various biological samples, which provides a novel approach to identify key metabolic biomarkers and pathways(Sun, 2019). Importantly, due to the homeostatic alteration in the body, a multitude of abnormal lipid metabolic activities were observed during the progression of ischemic stroke(Au, 2018). In our study, a systemic lipidomics study based on UHPLC-QTOF-MS has certain significance for studying the intervention mechanism of myriocin in the pathophysiology of cerebral I/R injury. We also determined the expressions of relevant lipid metabolism-related genes by real-time quantitative polymerase chain reaction (RT-qPCR) analysis. In addition, the underlying apoptosis mechanism of myriocin from the point of lipid metabolites was further explored.

Materials And Methods

Chemicals and reagents

Myriocin (purity>98%, B6064) was purchased from APExBIO (Houston, TX, USA). MTBE, methanol, acetonitrile and dichloromethane of LC-MS grade were purchased from Merck (Darmstadt, Germany). Ultrapure water was purified from Milli-Q system (Billerica, MA, USA)

Experimental animals and drug administration

Male Sprague-Dawley rats weighing 250–300 g (SPF grade, license No. SCXK(Yu)2017-0001) were obtained from Experimental Animal Center of Zhengzhou University (Zhengzhou, China). Animal experiments were approved by the Ethics Committee of Zhengzhou University. The animals were housed with free water and diet in colony cages on a 12h light/dark cycle. Rats were randomly assigned into three groups with 20 rats for each group: the sham group, the I/R group and the myriocin-treated group.

Cerebral ischemia/reperfusion rat model was performed by middle cerebral artery occlusion (MCAO) as previously described (Mavroudakis, 2020). In brief, the left middle cerebral artery (MCA) of rats was occluded by inserting a 5–0 monofilament long nylon suture into the ICA for 2 hours, and then to reperfusion for 22 hours. Rats in I/R and myriocin group were performed with ischemia/reperfusion surgery, while the sham group received the same surgical procedure except there was no thread insertion.

Myriocin was administered intraperitoneally for 7 days with 0.3 mg/kg dissolved in DMSO before MCAO in rats. The sham and model groups were given an equal volume of dimethylsulfoxide (DMSO) for injection in the same way.

Sample preparation and lipid extraction

After the behavioural assessment, rats were sacrificed and the ischemic side of cerebral cortical tissue samples were quickly extracted. Total lipids are extracted from brain homogenate using a modified Folch method (Orei et al., 2012). Briefly, the brain tissues (n=6 per group) were weighed precisely (50.0±0.5mg) and then 1mL of chloroform/methanol (2:1, v/v) was added. The mixture was added ice-cold water to induce phase separation, and then centrifuged at 13,000 rpm for 10 min. Next, the layer containing chloroform was collected and dried under a stream of N2. Finally, the extracts were reconstituted in acetonitrile for further lipid analyses. Meanwhile, quality control (QC) samples were prepared by mixing equivalent lipid extracts of each cerebral cortical tissue and injected every six samples during the analysis to monitor the stability of the system and the method.

The untargeted lipidomic analysis was carried out using AB Sciex ExinLC^{TM} UHPLC system (Framingham, MA, USA) with AB Sciex Triple-TOF^{TM} 5600^{+} mass spectrometer (Framingham, MA, USA). Samples were injected on an Acquity UPLC®BEH C18 column (2.1mm× 100 mm,1.7 μm, Waters, Milford, MA) that was used with the injection volume of 5 μL. The column temperature was 35°C and flow rate was 0.4 mL/min. The mobile phase consisted of 0.1% formic acid in water (solvent A) and 0.1% formic acid in acetonitrile (solvent B). The gradient conditions were as follows:0–3 min with 5–22% B; 3–12 min with 22–60% B; 12–16 min with 60–70% B; 16–22 min with 70-100% B; 23-25 min with 5% B.

Mass spectrometry (MS) analysis was performed with an electrospray ionization (ESI) source in both positive and negative ion modes. ESI source conditions were set as follows: the nebulizer gas pressure was set to 60 psi, the curtain gas was 30 psi, the temperature was 550°C, the full scan data ranged from 100 to 1000 m/z and the collision energy was 35 eV in positive mode and negative mode.

Evaluation of neurological function and cerebral infarct volume

Neurological deficits were assessed at 24h after reperfusion with Zea Longa 5-point scale(Longa et al., 1989) to evaluate the MCAO model. Briefly, 0 points, no neurological deficit; 1 point, forelimb flexion; 2 points, circling to the contralateral side; 3 points, falling towards the contralateral side when walking; and 4 points, difficult to walk. The higher score represents the more severe behavior disorder in rats. Model was considered successful when the score was 1–3. Brains (n=3 per group) were quickly placed on ice and cut into five transverse slices. After that the brain slices were stained with 2% TTC (2,3,5-triphenyltetrazolium chloride, Sigma) at 37°C for 30 min, and then fixed in 4% paraformaldehyde for overnight. All stained slices were photographed and the infarct volume was quantified by Image-pro plus 6.0 software.

Nissl staining and TUNEL staining

Nissl staining was performed to evaluate the morphological changes in the brain. According to previously described methods(Zhang et al., 2002), the rat brain tissues were fixed in 4% paraformaldehyde fixed overnight, embedded in paraffin and cut into coronal sections. The brain sections were stained with Nissl staining solution (Beyotime, China) and observed under a fluorescence microscope (magnification 200×). The TUNEL Apoptosis Assay Kit (Beyotime, China) was used to examine cell apoptosis in rat brain tissue for TUNEL staining. Briefly, nuclei were stained by DAPI dye after TUNEL staining. Then the brain sections were observed under a fluorescence microscope and the cells with green fluorescence were considered as apoptotic cells. Quantification of positive cells was performed by Image J software. TUNEL-positive cells (%) = (apoptotic cells/total cells) × 100%.

Reverse transcription-quantitative PCR (RT-qPCR) analysis

Total RNA was extracted from the cerebral cortex tissue with Trizol reagent (Invitrogen, USA) and then reversely transcribed to cDNA using PrimeScript RT reagent (Thermo Fisher Scientific, USA), and real-time PCR was performed in triplicate using SYBR Green PCR Master Mix (Applied Biosystems). The amplification procedures were as follows: 95°C for 10 min denaturation, followed by 40 cycles of 95°C for 15 s, and 60°C for 60s. Data were measured using the $2^{-\Delta\Delta Ct}$ method using GAPDH as the reference gene. All gene analyses were done at least three times. The primer sequences used for RT-qPCR are listed in Table S1.

Western blot analysis

Equal amounts of denatured protein (40μg) were separated by electrophoresis on 12% SDS-PAGE, and then transferred to a PVDF membrane (Millipore, USA). A total of 5% nonfat milk was used for blocking at room temperature. The primary antibodies used in the present study were as follows: SPTLC1(sc-136076,Santa Cruz), SPTLC2

(sc-398704,Santa Cruz), Bcl-2 (ab196495, Abcam), Bax (ab32503, Abcam), caspase-3 (9662s, CST), cleaved-caspase-3 (9664s, CST) and GAPDH (AF7021, Affinity). Primary antibodies were used to incubate overnight at 4°C. After being washed three times with TBST, the membranes were next incubated with appropriate secondary antibodies for 1 hour at room temperature. GAPDH served as an internal control. The membranes were analyzed with Bio-Rad ChemiDoc system and protein amount was quantified by Image J software.

Statistical analysis and multivariate data analysis

GraphPad Prism 8.3 (GraphPad Prism Software, San Diego, CA, USA) software were used for statistical analysis. The data were analysed using one-way ANOVA for multiple group comparisons. All data were expressed as the mean ± SE (standard error). Values with $P < 0.05$ were considered significant.

ProteoWizard software converted the original data into mzXML format, and then off-line XCMS software was used for peak alignment, retention time correction, and peak area extraction. The data matrices after 80% principle screening and normalization were input into SIMCA-P 14.1 software (Umetrics, Sweden) for multivariate analysis, including principal component analysis (PCA) and orthogonal partial least squares

discriminant analysis (OPLS-DA). The cross-validation parameters R^2 and Q^2 values were applied to assess the model. In addition, the OPLS-DA models were validated by the response values of the 200 permutation tests, which was applied to prevent overfitting. Variable importance for the projection (VIP) values was obtained from the OPLS-DA. The selected metabolites data were performed with Metaboanalyst 5.0 (http://www.metaboanalyst.ca/) used for potential metabolic pathway analysis and clustering heatmap analysis.

Results

Myriocin attenuated ischemic brain damage in rats

To evaluate the protective effect of myriocin on cerebral I/R model, Neurological scores and TTC staining were performed to assess neurological function and infarct volume, respectively. As showed in Fig. 2A, the neurological scores of the I/R group were markedly increased compared to sham group (P<0.05). Compared with the I/R group, myriocin treatment decreased the neurological defect scores (P<0.05). After staining with 2% TTC solution, the normal brain tissue of each group was stained red while the infarct area was pale (Fig. 2B). The quantitative statistical results of infarct volumes showed that the cerebral infarct volume in I/R group was increased significantly compared to sham group (Fig. 2C, P<0.05). Compared with the I/R group, myriocin treatment attenuated the infarct volume (P<0.05).

Nissl staining showed the pathological changes of the ischemic area in cerebral I/R model rats. As shown in Fig. 2D, compared with the sham group, the I/R group showed neural cells were poorly arranged and became slightly swollen. Nissl bodies decreased markedly and some of the nucleoli were shrunken and deep stained. After intervention with myriocin, the neuron damage was significantly reduced (P<0.05).

Myriocin inhibited ceramide accumulation of the de novo synthesis pathway in the ischemia stroke area

In order to demonstrate that myriocin counteracts a pathological mechanism during cerebral ischemia/reperfusion damage, we assessed SPT enzyme expression, that is the target of myriocin. The qRT-PCR results showed that I/R significantly increased the mRNA levels of SPTLC2, and myriocin successfully decreased SPTLC2 mRNA among groups (Fig. 3A). Similarly, we found consistent results on SPTLC1 and SPTLC2 protein levels via Western blotting (Fig. 3B). Overall, the above finding suggested that ceramide accumulation induced through a transcriptional activation of the *de novo* synthesis pathway in cerebral I/R-injured rats, and myriocin could inhibit this effect.

Multivariate Statistical Analysis

UPLC-Q-TOF/MS acquired the lipid profiles of cerebral cortex samples. Fig. S1 showed a representative total ion chromatogram (TIC) of QC group in positive and negative ion modes. Multivariate statistical analysis of PCA and OPLS-DA were applied for revealing the lipid metabolic differences among the three groups. From the processed data, PCA analysis was used to distinguish the differential regulation of lipid

species between the compared groups according to the similarity of data. In our study, a clear separation between each group was observed in PCA score plots, and the QC samples displayed good aggregation (Fig. 4). The results showed that myriocin group was separated from the model group with approaching the sham group, indicating that cerebral I/R injury could be effectively reversed after myriocin intervention. Additionally, the OPLS-DA was used to analyze the data in order to further separate the differences between groups and facilitate subsequent search for potential biomarkers. The R^2 and Q^2 value are the interpretation rate and prediction capabilities of the established model, respectively. In our study, As can be seen from the scatter plots of OPLS-DA models established, the separation of Sham group and I/R group was obvious. Besides, the Myriocin group and the I/R group were clearly separated (Supplementary, Fig. S2A,C). Both R^2Y and Q^2 of the OPLS-DA models were above 0.8, indicating excellent predictive ability and reliability. Moreover, the 200 permutation tests was used to validate the performance of the OPLS-DA models, and there was no overfitting phenomenon (Supplementary, Fig. S2B, D)

Potential Biomarkers and Metabolic pathway analysis

The structure of the metabolites were determined with MS/MS information including m/z, retention time and characteristic fragments. Metabolites identified by comparing with authentic standard and database such as HMDB (http://www.hmdb.ca/), MassBank (http://www.massbank.jp/), and METLIN (http://metlin.scripps.edu/) and the database established by ourselves. When VIP >1and $P<0.05$, the metabolites were exhibited statistically significant, which were identified as potential biomarkers. A total of 15 potential biomarkers were finally selected, as listed in Table 1. Compared with the sham group, there were six different lipid metabolites that were significantly up-regulated in the I/R group ($P<0.05$), including Cer (d18:1/16:0), Cer (d18:1/18:0), Cer (d18:0/18:0), C18 Sphingosine, LPE (18:0) and LPC (20:4). The other nine different lipid metabolites were significantly down-regulated in the I/R group ($P<0.05$). After myriocin treatment, all above 15 lipid metabolic disturbances were effectively ameliorated.

Table 1
Detailed information of differential lipid biomarkers identified by UPLC-Q/TOF-MS

No.	Metabolites	t_R/min	Ion(m/z)	type	PubChem	trend	
						I/R/Sham	Myriocin/I/R
1	Cer(d18:1/16:0)	8.67	538.4	$[M-H]^-$	5283564	↑**	↓**
2	Cer(d18:1/18:0)	9.45	564.4	$[M-H]^-$	5283565	↑**	↓**
3	Cer(d18:1/24:1)	10.23	594.4	[M□H]□	5283566	↓*	↑*
4	Cer(d18:0/18:0)	9.45	568.6	$[M-H]^-$	5283573	↑*	↓*
5	C18 Sphingosine	6.13	281.3	[M□H]□	-	↑**	↓**
6	SM(d18:0/18:0)	8.58	731.6	$[M-H]^-$	44260130	↓**	↑**
7	SM(d18:0/20:0)	9.41	759.6	[M□H]□	44260131	↓**	↑*
8	LPE(18:0)	4.81	480.31	$[M-H]^-$	53480667	↑**	↓**
9	LPC(20:4)	2.81	602.35	$[M-H]^-$	24779476	↑**	↓**
10	DAG(16:0/18:1)	10.04	612.6	$[M-H]^-$	9543972	↓*	↑**
11	PE(P-18:0/20:1)	9.97	754.6	[M□H]□	52925086	↓*	↑*
12	PE(16:0/22:6)	8.51	762.51	[M□H]□	5283497	↓*	↑*
13	PC(16:0/18:1)	7.75	818.5	$[M-H]^-$	24778688	↓**	↑**
14	PC(18:1/18:1)	8.79	844.61	[M□H]□	6437081	↓*	↑**
15	PC(18:0/20:4)	8.02	868.61	$[M-H]^-$	16219824	↓**	↑*
Arrow (↑) represented increase in I/R group compared to sham group;							
Arrow (↓) represented decrease in myriocin group compared to I/R group;							
*, **, and *** indicate $P < 0.05$, $P < 0.01$, respectively							
Abbreviations::Cer, ceramide; SM, sphingomyelin; PC, phosphatidylcholine; PE, phosphatidylethanolamine; LPC, lysophosphatidylcholine; LPE, lysophosphatidylethanolamine; DAG, diacylglycerol;							

The pathways of potential biomarkers were analyzed using MetaboAnalyst 5.0 related to metabolic pathway enrichment analysis. The detailed information of the metabolic pathways was shown in Table S2. Clustering heatmap was conducted to more visually exhibit the trend of the variation of 15 differential metabolites among the three groups. The obtained clustering results in the form of heatmap were shown

in Fig. 5A. Each little square represents a sample as well as red represents the increase and blue represents the decrease in intensity, respectively. As demonstrated in Fig. 5B, the most relevant metabolic pathways regulated by myriocin against cerebral I/R injury is sphingolipid metabolism and glycerophospholipid metabolism with the impact value > 0.1.

Myriocin influenced the expression levels of enzymes genes involved in the pathways of altered metabolites

To investigate the role of myriocin in sphingolipid and glycerophospholipid metabolism, we determined the expression of relevant enzymes involved in cerebral I/R injury in rats, including ASMase, NSMase, SGMS1, SGMS2, ASAH1, ASAH2, ACER2, ACER3 and PLA2 by RT-qPCR analysis. As a result, eight showed differentially changed expression profiles among the nine genes. Fig. 6 showed that the mRNA expression levels of ASMase, NSMase, SGMS2, ASAH1, ACER2, ACER3 and PLA2 were up-regulated obviously, while SGMS1 were down-regulated drastically in the I/R group when compared with the sham group. Upon the myriocin treatment, the mRNA levels of ASMase, NSMase, SGMS2, ASAH1, ACER2, ACER3 and PLA2 were all significantly decreased and SMS2 were increased when compared with the I/R group (P<0.05). However, the level of ASAH2 showed no significant difference among groups.

Myriocin inhibited relative apoptotic molecular expression levels

TUNEL staining was adopted to quantify the number of TUNEL-positive cells from the rat cerebral cortex. The results showed that compared with the sham-operated rats, apoptotic cells in the I/R group was significantly increased and significantly decreased after myriocin treatment (Fig. 7A, B). Moreover, to further explore the potential anti-apoptotic mechanism induced by myriocin, we next estimate/d the protein expression of the apoptosis-related proteins by western blot analysis (Fig. 7C, D). The results showed that Myriocin decreased the protein expressions of Bax, caspase-3, cleaved-caspase-3 and increased the protein expressions of Bcl-2 compared with the I/R group (P<0.05). These results suggested that myriocin inhibited apoptosis in cerebral cortex of rats with cerebral I/R.

Discussion

Collectively, lipidomics and gene expression analysis indicated that myriocin treatment induced complex responses from multiple interconnected metabolic pathways (Fig. 8). We can better understand the potential causal mechanisms of cerebral I/R injury in rats by analyzing the metabolic network.

Initially, in this study we verified that myriocin could significantly decrease cerebral infarction, neurological deficits and pathological changes in cerebral I/R rats. It is interesting to note that myriocin was found to significantly reduce SPTLC2 but not SPTLC1 after myriocin administration, indicating that SPTLC2 is more critical under the cerebral ischemia conditions.The above studies showed that myriocin

could effectively ameliorate SPTLC2 activity in the cerebral ischemic cortex, providing stable samples for consequent lipidomics analysis.

Sphingolipids play a critical physiological role in maintaining the structure of cell membranes and are extensively involved in regulating various biological signal transduction processes, such as cell growth, apoptosis, and signal transduction(Grösch et al., 2018; Sun et al., 2016). Meanwhile, sphingolipids are mainly composed of ceramide (Cer), sphingomyelin (SM) and sphingosine(Hannun et al., 2001). Among these lipids, ceramide is the central component of sphingolipid metabolism, which is emerged as a second messenger involved in regulating the physiological activities and metabolism of cells (Hannun and Obeid, 2008).The accumulation of ceramide in the pathogenetic mechanism of cerebral I/R injury has been observed in previous associated studies, which is consistent with our observation(Liu et al., 2000; Takahashi et al., 2004; Yu et al., 2007). In our study, we found that several long-chain Ceramide, Cer (d18:1/16:0) and Cer (d18:1/18:0), were significantly increased in the I/R group when compared with the sham group. However, notably, we also found the very-long-chain ceramide, Cer (d18:1/24:1), was markedly decreased in the I/R group. Our data showed that myriocin could improve the disturbances of these three ceramides in I/R group. It has been reported in the literature that distinct chain lengths of ceramide that synthesized by different ceramide synthases regulated different physiological processes(Cha et al., 2016; Chan and Goldkorn, 2000).Thus, we believe that different ceramide species showed different responses to ischemic injury, but further researches are required.

Ceramide levels are regulated by complex metabolic pathways, in the research, we tried to clarify the effects of inhibition the *de novo* synthesis of Cer by myriocin on other metabolic mechanisms of Cer in rats with cerebral I/R injury. Ceramide is produced from sphingomyelin (SM) hydrolysis by sphingomyelinases (SMases), along with this, ceramide is converted to sphingomyelin by sphingomyelin

synthase(SGMS)(Tian et al., 2009). Moreover, in brain tissue, ceramides are hydrolyzed into sphingosine under the action of ceramidase encoded by four different genes, which are acid ceramidase(ASAH1)、neutral ceramide (ASAH2), alkaline ceramidase2 (ACER2), and alkaline ceramidase3 (ACER3). In our results, a decreased trend of SM(d18:0/18:0) and SM(d18:0/20:0) was observed after cerebral I/R injury in rats. Additionally, there was a concomitant rise in C18 Sphinganine levels in the I/R group, which is consistent with previous literature reports (Sun et al., 2010). In the present study, we detected that key sphingomyelin cycle-related enzyme (ASMase, NSMase) mRNA expression levels tended to increase and SGMS1 mRNA expression levels tended to decrease after cerebral I/R injury in rats, which explains the reduction in ceramide/sphingomyelin ratio. Similarly, in view of the increased ceramide conversion-related enzyme (ASAH1, ACER2, ACER3) mRNA expressions after cerebral I/R injury in rats, it may account for the accumulation of C18 sphingosine.Remarkably, myriocin could ameliorate the dysregulation of sphingolipid metabolism at the level of the above metabolic enzyme genes, as compared to untreated animals.

Meanwhile, another finding in this study is that an increasing level of DAG (16:0/18:1) was observed in I/R group. It has been shown that SMS enzymes convert Cer and phosphatidylcholine (PC) into SM and

diacylglycerol (DAG), respectively. According to our result, a higher level of DAG (16:0/18:1) might be associated with increased mRNA expression of SMS2, which needs to be further investigated.

Glycerophospholipids are the principal lipid components of biological membranes, which are involved in diverse signal transduction processes such as apoptosis and membrane fusion(Farooqui et al., 2000). In animal tissues, phosphatidylcholine (PC) and phosphatidylethanolamine (PE) are the most abundant and important intermediates in glycerolphospholipid metabolism(Vance, 2015). In our study, PC (16:0/18:1), PC (18:1/18:1), PC (18:0/20:4), PE(P-18:0/20:1), and PE (16:0/22:6) was significantly decreased, whereas LPC (20:4) and LPE (18:0) was significantly increased in the I/R group. After myriocin treatment, the levels of these metabolites showed a trend toward the normal status. Liu et al(Liu et al., 2017)identified PC(5:0/5:0) and LysoPE(18:2) showed great potential to serve as biomarkers of distinguishing acute ischemic stroke patients from healthy individuals. Rabiei and colleagues (Rabiei et al., 2013)found that the PC content was inversely associated with infarct volumes in a rat model of focal cerebral ischemia injury, which strongly supported the role of PC in ischemic injury. Phospholipids and lysophospholipids can convert to each other through the “Lands cycle” to maintain lipid homeostasis(Wu et al., 2016). When activation of phospholipase A2 (PLA2), PC and PE in organisms can be catalyzed hydrolysis to produce the corresponding single-stranded lysophospholipids LPC and LPE, respectively. Previous reports has been demonstrated that activation of PLA2 plays a pivotal role in acute cerebral ischemia linked to neuronal cell death, which is in line with the results of our study (Sun et al., 2009). Notably, we showed that myriocin could ameliorate the dysregulation of glycerophospholipid metabolism as a result of PLA2, which are related with the balance of land cycle in the cerebral I/R model rats .

Importantly, apoptosis is the key factors of neuronal cell death in cerebral I/R injury (Radak et al., 2017). It is recognized that sphingolipids like ceramides are known to be involved in apoptosis (Hannun, 1996). Based on our present results, we speculated that ceramide causes apoptosis-induced cell death in cerebral I/R injury. We observed the morphological changes of neuronal cells in the cortical brain regions through TUNEL staining, validating our hypothesis. Then, we further explored the underlying mechanisms of myriocin on inhibiting cortical neuronal apoptosis. Our results clearly confirmed that myriocin downregulated the protein levels of Bax, caspase-3 and cleaved caspase-3 while upregulating Bcl-2, thus promoting the survival of neural cells after cerebral ischemia.

However, it is a limitation that this study determined only the mRNA expressions of enzymes. Thus, the enzyme protein levels will be further measured.

Conclusions

Taken together, the present work provides a new perspective for a systematic study of the therapeutic effects of myriocin in ischemia stroke. UPLC-Q-TOF/MS-based lipidomics approach was firstly applied in the present study to elucidate the neuroprotective effect of myriocin against cerebral I/R injury. Combined lipidomics and RT-qPCR analysis results, the study revealed that myriocin could improve the disruption of 15 lipid metabolites by regulating the expression of relevant enzyme genes in cerebral cortical tissue of

rats. Moreover, the results further verified that myriocin inhibited apoptosis induced by cerebral I/R injury. Therefore, the findings of this study suggested that myriocin might be serve as a potential new therapeutic target to alleviate cerebral I/R injury.

Declarations

Data Availability The data generated during the current study are available from the corresponding author upon request.

Ethical Statement:

Ethics Approval The animal experiments were approved by the Institutional Animal Care and Animal Ethics Committee of Zhengzhou University.

Consent to Participate Not Applicable

Consent for Publication All authors agreed to publication.

Availability of Data and Materials The data and materials generated during the current study are available from the corresponding author upon request.

Conflict of Interests The authors declare no competing financial interest.

Funding This work was supported by the Key Scientific Research Project in Colleges and Universities of Henan Province (Grant No.19A360033); The Science and Technology Department of Henan Province (Grant No.182102310169, No.182102310540); The authors are grateful to these institutions for the financial support.

Authors' Contributions Y.L. and D.L. conceived and designed the study; T.W. performed the experiments and drafted the manuscript; J.Z. and M.Y. contributed to acquisition of data or analysis data; J.G. was responsible for editing; Y.L. and D.L.reviewed the manuscript. All authors approved the final manuscript.

Acknowledgments Not Applicable

References

1. Au A (2018) Metabolomics and Lipidomics of Ischemic Stroke. Adv Clin Chem 85:31–69
2. Bhuiyan M, Jung SY, Yoo H, Lee Y, Jin C (2010) Involvement of ceramide in ischemic tolerance induced by preconditioning with sublethal oxygen-glucose deprivation in primary cultured cortical neurons of rats. Biol Pharm Bull 33:11–17
3. Bonezzi F, Piccoli M, Dei Cas M, Paroni R, Mingione A, Monasky MM, Caretti A, Riganti C, Ghidoni R, Pappone C, Anastasia L, Signorelli P (2019) Sphingolipid Synthesis Inhibition by Myriocin

Administration Enhances Lipid Consumption and Ameliorates Lipid Response to Myocardial Ischemia Reperfusion Injury. Front Physiol 10:986

4. Cas MDZ, Mingione A, Caretti A, Ghidoni A, Signorelli R, Paroni P, R (2020) An Innovative Lipidomic Workflow to Investigate the Lipid Profile in a Cystic Fibrosis Cell Line. Cells 12:1197
5. Cha HJ, He C, Zhao H, Dong Y, An I, An S (2016) Intercellular and intracellular functions of ceramides and their metabolites in skin (Review). Int J Mol Med 38:16–22
6. Chan C, Goldkorn T (2000) Ceramide path in human lung cell death. Am J respiratory cell Mol biology 22:460–468
7. Cheng C-YL (2016) Y., Anti-Inflammatory Effects of Traditional Chinese Medicines against Ischemic Injury in In Vivo Models of Cerebral Ischemia. Evidence-based Complementary Alternative Medicine: eCAM 2016
8. Doria MLC, Macedo Z, Simões B, Domingues C, Helguero P, Domingues L, M (2011) Lipidomic approach to identify patterns in phospholipid profiles and define class differences in mammary epithelial and breast cancer cells. Breast Cancer Research Treatment 133:635–648
9. Farooqui AA, Horrocks L, Farooqui T (2000) Glycerophospholipids in brain: their metabolism, incorporation into membranes, functions, and involvement in neurological disorders. Chem Phys lipids 106:1–29
10. Fitzner DB, Penkert JM, Bergner H, Su CG, Weil M, Surma M, Mann MA, Klose M, Simons C, M (2020) Cell-Type- and Brain-Region-Resolved Mouse Brain Lipidome. Cell Rep 32:108132
11. Fyrst HS, J (2010) An update on sphingosine-1-phosphate and other sphingolipid mediators. Nat Chem Biol 6:489–497
12. Grösch S, Alessenko A, Albi E (2018) The Many Facets of Sphingolipids in the Specific Phases of Acute Inflammatory Response. Mediat. Inflamm 2018
13. Hannun Y, Luberto C, Argraves KM (2001) Enzymes of sphingolipid metabolism: from modular to integrative signaling. Biochemistry 40:4893–4903
14. Hannun Y, Obeid L (2008) Principles of bioactive lipid signalling: lessons from sphingolipids. Nat Rev Mol Cell Biol 9:139–150
15. Hannun YAJS (1996) Functions of Ceramide in Coordinating Cellular Responses to Stress. 274:1855–1859
16. Khandelwal PY, Sacco D,R (2016) Sacco, R. Acute Ischemic Stroke Intervention. J Am Coll Cardiol 67:2631–2644
17. Lai TZ, Wang S, Y (2014) Excitotoxicity and stroke: Identifying novel targets for neuroprotection. Prog Neurobiol 115:157–188
18. Lee Y-SC, Choi K-M, Ji M-H, Lee S-Y, Sin S, Oh D-M, Lee K, Hong Y-M, Yun J, Yoo Y, H (2011) Serine palmitoyltransferase inhibitor myriocin induces growth inhibition of B16F10 melanoma cells through G2/M phase arrest.Cell Prolif44

19. Liu J, Ginis I, Spatz M, Hallenbeck J (2000) Hypoxic preconditioning protects cultured neurons against hypoxic stress via TNF-alpha and ceramide. Am J Physiol 278:C144–153
20. Liu P, Li R, Antonov AA, Wang L, Li W, Hua Y-f, Guo H, Wang L, Liu P, Chen L, Tian Y, Xu F, Zhang Z, Zhu Y, Huang Y (2017) Discovery of Metabolite Biomarkers for Acute Ischemic Stroke Progression. J Proteome Res 16:773–779
21. Longa EZ, Weinstein PR, Carlson S, Cummins RJS (1989) circulation, a.j.o.c., Reversible middle cerebral artery occlusion without craniectomy in rats. 20, 84
22. Mavroudakis LS, Duncan SL, Stenzel-Poore KD, Laskin MP, Lanekoff J, I (2020) CpG preconditioning reduces accumulation of lysophosphatidylcholine in ischemic brain tissue after middle cerebral artery occlusion. Analytical Bioanalytical Chemistry
23. Naudí AC, Jové R, Ayala M, Gonzalo V, Portero-Otín H, Ferrer M, Pamplona I, R (2015) Lipidomics of human brain aging and Alzheimer's disease pathology. Int Rev Neurobiol 122:133–189
24. Novgorodov SR, Keffler CL, Yu JA, Kindy J, Macklin M, Lombard W, Gudz D (2015) T., SIRT3 Deacetylates Ceramide Synthases. The Journal of Biological Chemistry. 291, 1957 - 1973
25. Obadia NL, Daliry M, Silvares A, Gomes RR, Tibiriçá F, Estato E, V (2017) Cerebral microvascular dysfunction in metabolic syndrome is exacerbated by ischemia reperfusion injury. BMC Neurosci 18:67
26. Orei M, Sepp?Nen-Laakso T, Sun D, Jing T, Therman S, Viehman R, Mustonen U, Erp T, Hy?Tyl?Inen T, Thompson PJGM (2012) Phospholipids and insulin resistance in psychosis: a lipidomics study of twin pairs discordant for schizophrenia. 4:1
27. Peralta CJ-C, Gracia-Sancho M, J (2013) Hepatic ischemia and reperfusion injury: effects on the liver sinusoidal milieu. J Hepatol 59:1094–1106
28. Rabiei Z, Bigdeli MR, Mohagheghi F (2013) Effect of dietary virgin olive oil on infarct volume and brain ceramide, cerebroside and phosphatidylcholine levels in rat stroke model. journal of shahrekord university of medical sciences
29. Radak D, Katsiki N, Resanovic I, Jovanovic A, Sudar-Milovanovic E, Zafirovic S, Mousad SA, Isenovic ER (2017) Apoptosis and Acute Brain Ischemia in Ischemic Stroke. Curr Vasc Pharmacol 15:115–122
30. Reforgiato MR, Milano G, Fabrias G, Casas J, Gasco P, Paroni R, Samaja M, Ghidoni R, Caretti A, Signorelli P (2016) Inhibition of ceramide de novo synthesis as a postischemic strategy to reduce myocardial reperfusion injury. Basic Res Cardiol 111:12
31. Schaller BG, Jacobs R et al (2003) Invited commentary: Ischemic tolerance: a window to endogenous neuroprotection? Lancet, pp 1007–1008
32. Sun GY, Shelat P, Jensen MB, He Y, Sun A, Simonyi Á (2009) Phospholipases A2 and Inflammatory Responses in the Central Nervous System. NeuroMol Med 12:133–148
33. Sun N, Keep R, Hua Y, Xi G (2016) Critical Role of the Sphingolipid Pathway in Stroke: a Review of Current Utility and Potential Therapeutic Targets. Translational Stroke Research 7:420–438

34. Sun X, Liu C, Qian M, Zhao Z, Guo J (2010) Ceramide from sphingomyelin hydrolysis differentially mediates mitogen-activated protein kinases (MAPKs) activation following cerebral ischemia in rat hippocampal CA1 subregion. J Biomedical Res 24:132–137
35. Sun YS, Saito K, Y (2019) Lipid Profile Characterization and Lipoprotein Comparison of Extracellular Vesicles from Human Plasma and Serum. Metabolites 9.
36. Takahashi K, Ginis I, Nishioka R, Klimanis D, Barone F, White RF, Chen Y, Hallenbeck J (2004) Glucosylceramide Synthase Activity and Ceramide Levels are Modulated during Cerebral Ischemia after Ischemic Preconditioning. J Cereb Blood Flow Metabolism 24:623–627
37. Tian H, Qiu T, Zhao J, Li L, Guo J (2009) Sphingomyelinase-induced ceramide production stimulate calcium-independent JNK and PP2A activation following cerebral ischemia. Brain Inj 23:1073–1080
38. Vance J (2015) Phospholipid Synthesis and Transport in Mammalian Cells.Traffic16
39. Wadsworth JM, Clarke DJ, McMahon SA, Lowther JP, Beattie AE, Langridge-Smith PR, Broughton HB, Dunn TM, Naismith JH, and Campopiano D. J (2013) The chemical basis of serine palmitoyltransferase inhibition by myriocin.J. Am. Chem. Soc.,14276–14285
40. Wu H, Bogdanov M, Zhang Y, Sun K, Zhao S, Song A, Luo R, Parchim N, Liu H, Huang A, Adebiyi MG, Jin J, Alexander DC, Milburn M, Idowu M, Juneja H, Kellems R, Dowhan W, Xia Y (2016) Hypoxia-mediated impaired erythrocyte Land “Cycle is pathogenic for sickle cell disease. Scientific Reports 6.
41. Wu M-YY, Liao G-T, Tsai W-T, Cheng A, Cheng Y-L, Li P-W, Li C-Y, C.-J (2018) Current Mechanistic Concepts in Ischemia and Reperfusion Injury. Cell Physiol Biochem 46:1650–1667
42. Yu JN, Chudakova S, Zhu D, Bielawska H, Bielawski A, Obeid J, Kindy L, Gudz M, T (2007) JNK3 Signaling Pathway Activates Ceramide Synthase Leading to Mitochondrial Dysfunction*. J Biol Chem 282:25940–25949
43. Yu WG, Jin D, Liu W, Qi S-l, S (2018) Propofol Prevents Oxidative Stress by Decreasing the Ischemic Accumulation of Succinate in Focal Cerebral Ischemia Reperfusion Injury. Neurochem Res 43:420–429
44. Yu Z, Nikolova-Karakashian M, Zhou DC, Schuchman G, Mattson E, M (2007) Pivotal role for acidic sphingomyelinase in cerebral ischemia-induced ceramide and cytokine production, and neuronal apoptosis. J Mol Neurosci 15:85–97
45. Zhang X, Cui SS, Wallace AE, Hannesson DK, Corcoran MEJ (2002) Relations between brain pathology and temporal lobe epilepsy. 22:6052–6061J.o.N.t.O.J.o.t.S.f.N

Figures

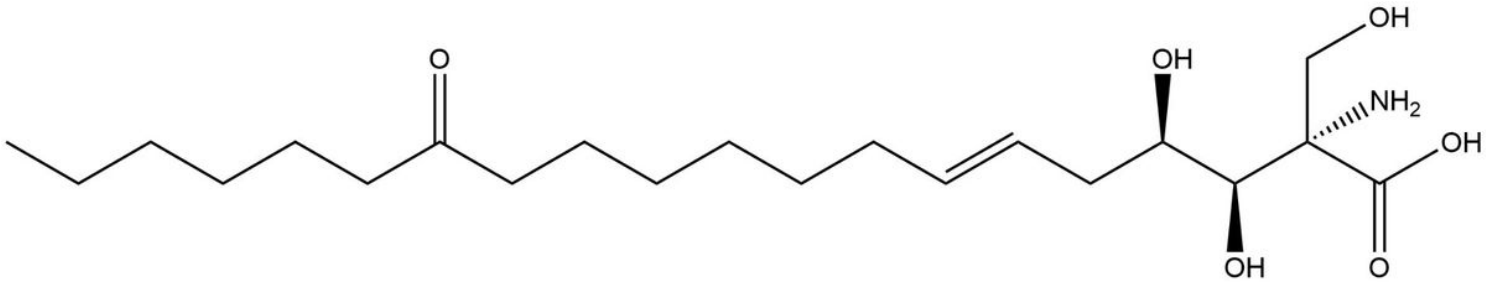

Figure 1

The chemical structure of myriocin.

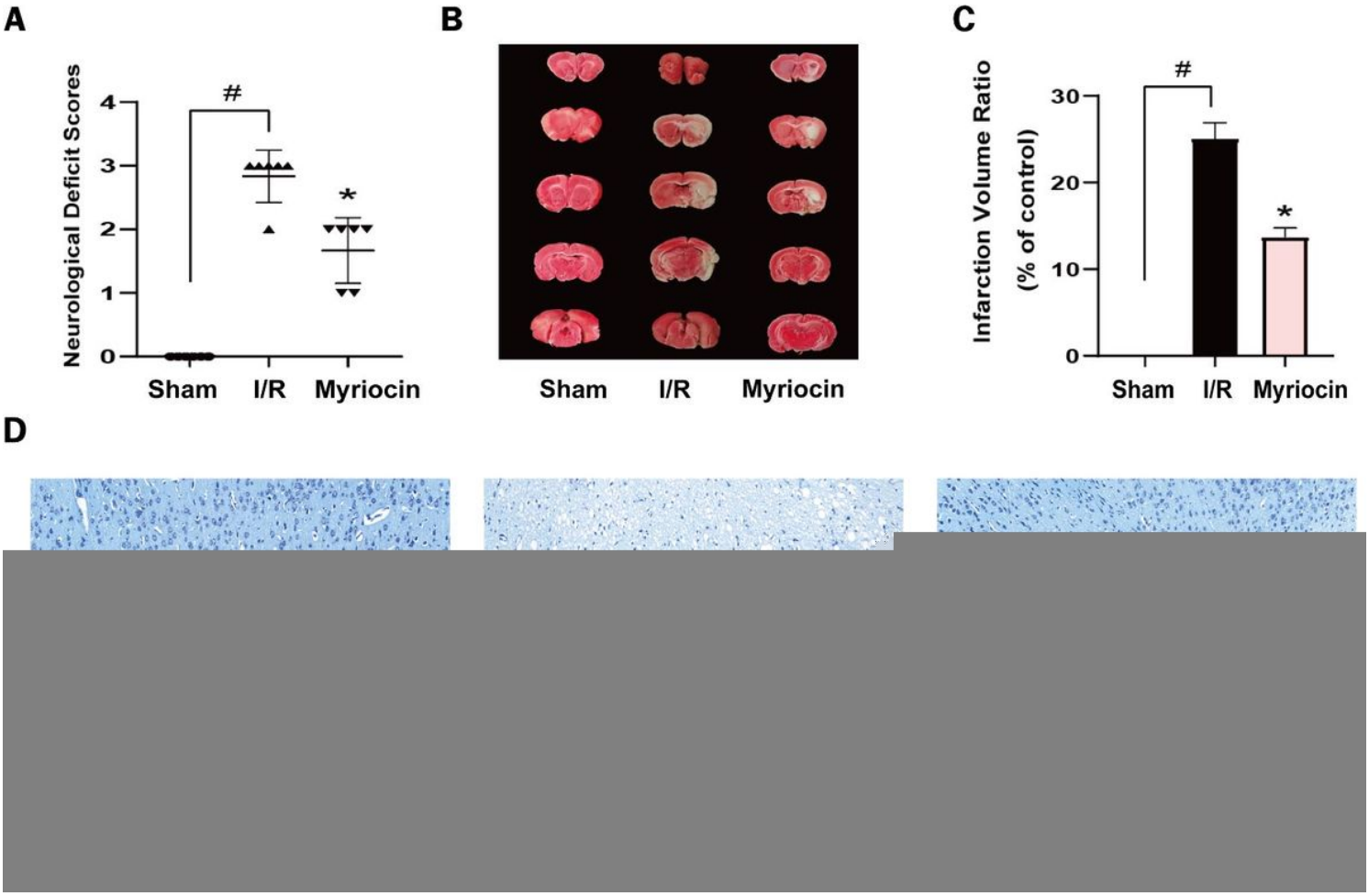

Figure 2

Myriocin played protective effects against cerebral I/R injury in rats. (A) Neurological deficit scores were assessed after 24 h of rat cerebral I/R (n=6). (B) Percentage of infarct volume in whole cerebral tissue. (n=3) (C) TTC staining of the brain tissue. (D) Observation of pathological changes by Nissl's staining in each group (magnification 200×, n=3). Data are expressed as the mean ± SD. Compared with the sham group, $^{\#}P<0.05$; Compared with the I/R group, $^{*}P<0.05$.

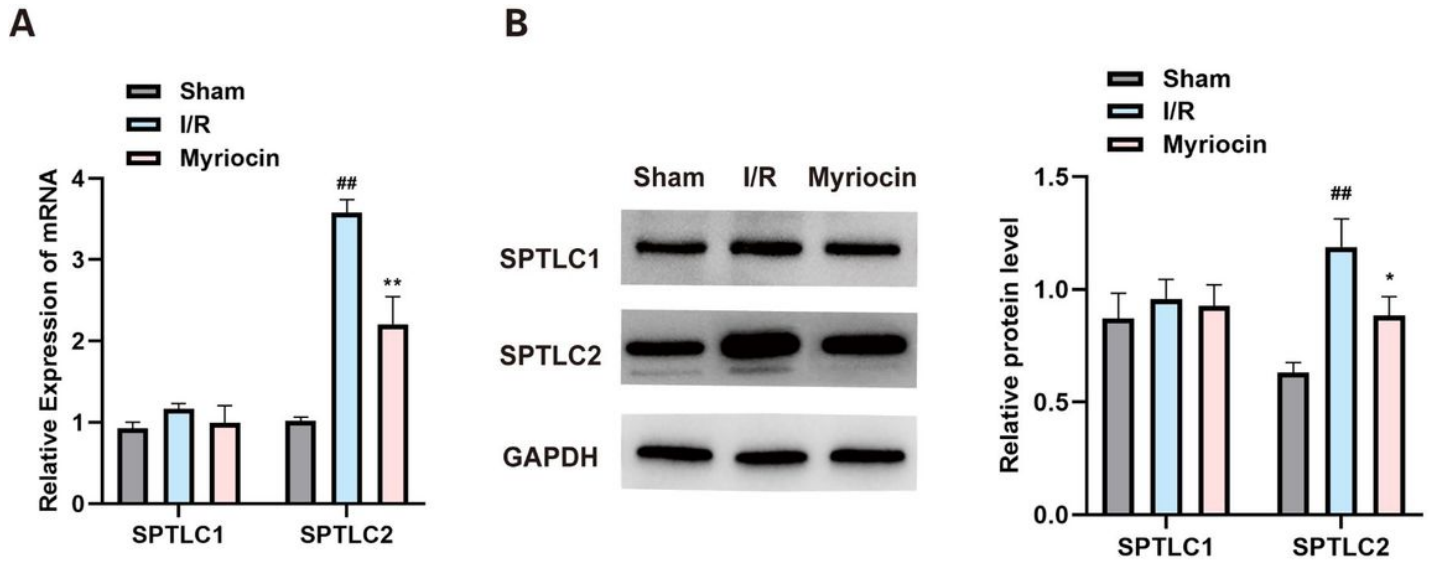

Figure 3

Myriocin inhibited ceramide accumulation of the *de novo* synthesis pathway in the ischemia stroke area. (A) Relative mRNA levels of SPTLC1 and SPTLC2 of each group were determined by quantitative real-time.(B) Protein levels of SPTLC1 and SPTLC2 of each group detected by western blot.GAPDH was used as an internal control. Data are presented as mean ± SD (n=3). Compared with the Sham group, $^{\#\#}P <$ 0.01; Compared with the I/R group $^{*}P <$0 .05, $^{**}P <$ 0.01.

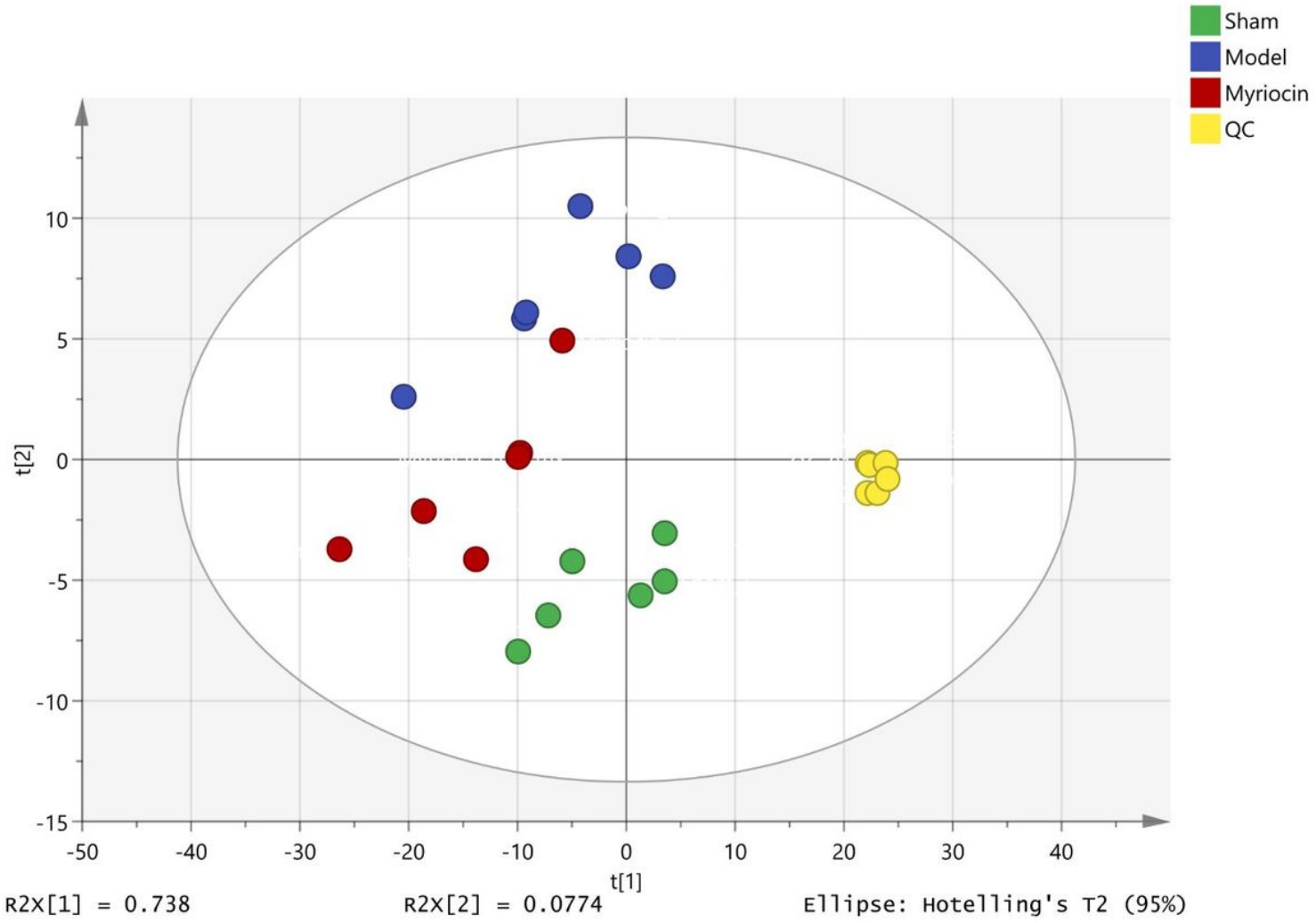

Figure 4

PCA scores plot of rat cerebral cortical tissues among the Sham, I/R, Myriocin and QC groups.

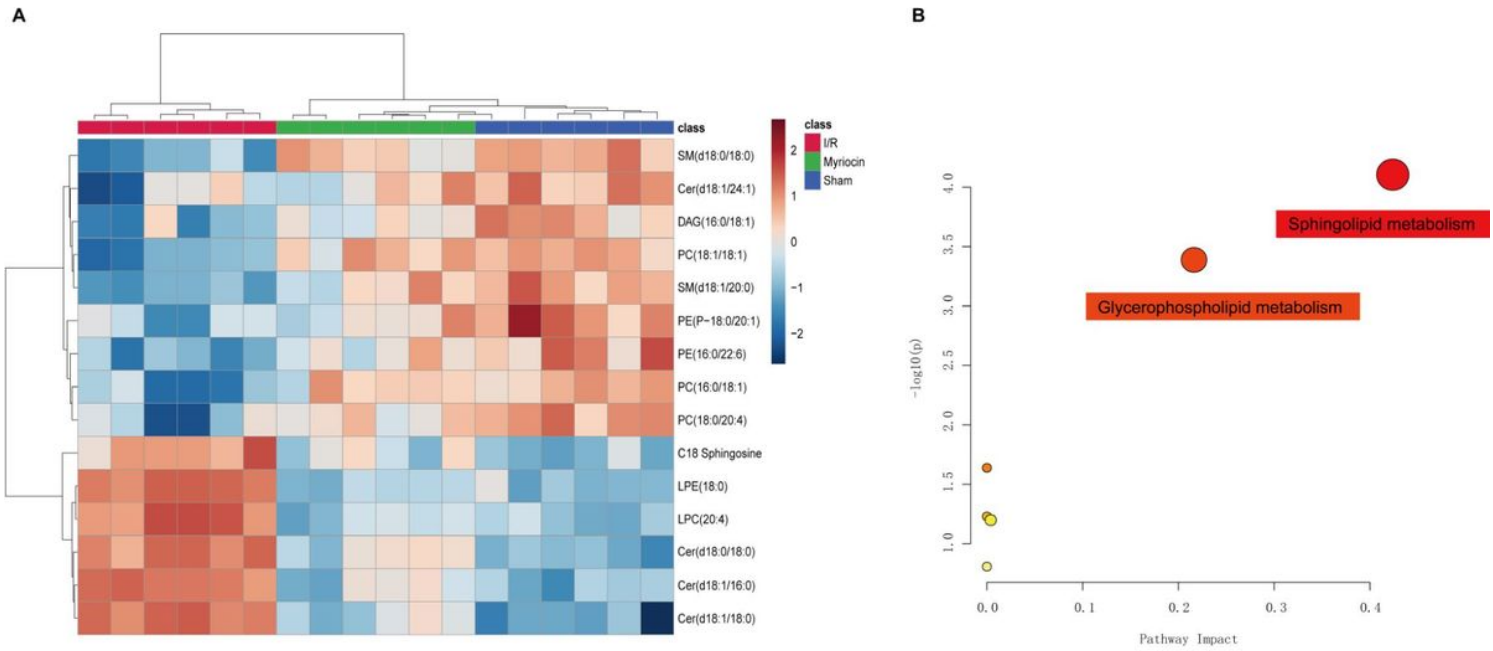

Figure 5

Potential biomarkers and metabolic pathway analysis. (A) Heatmap visualization of key metabolite expression of the brain regulated by the myriocin. (B) Metabolic pathway enrichment analysis of the brain regulated by the myriocin.

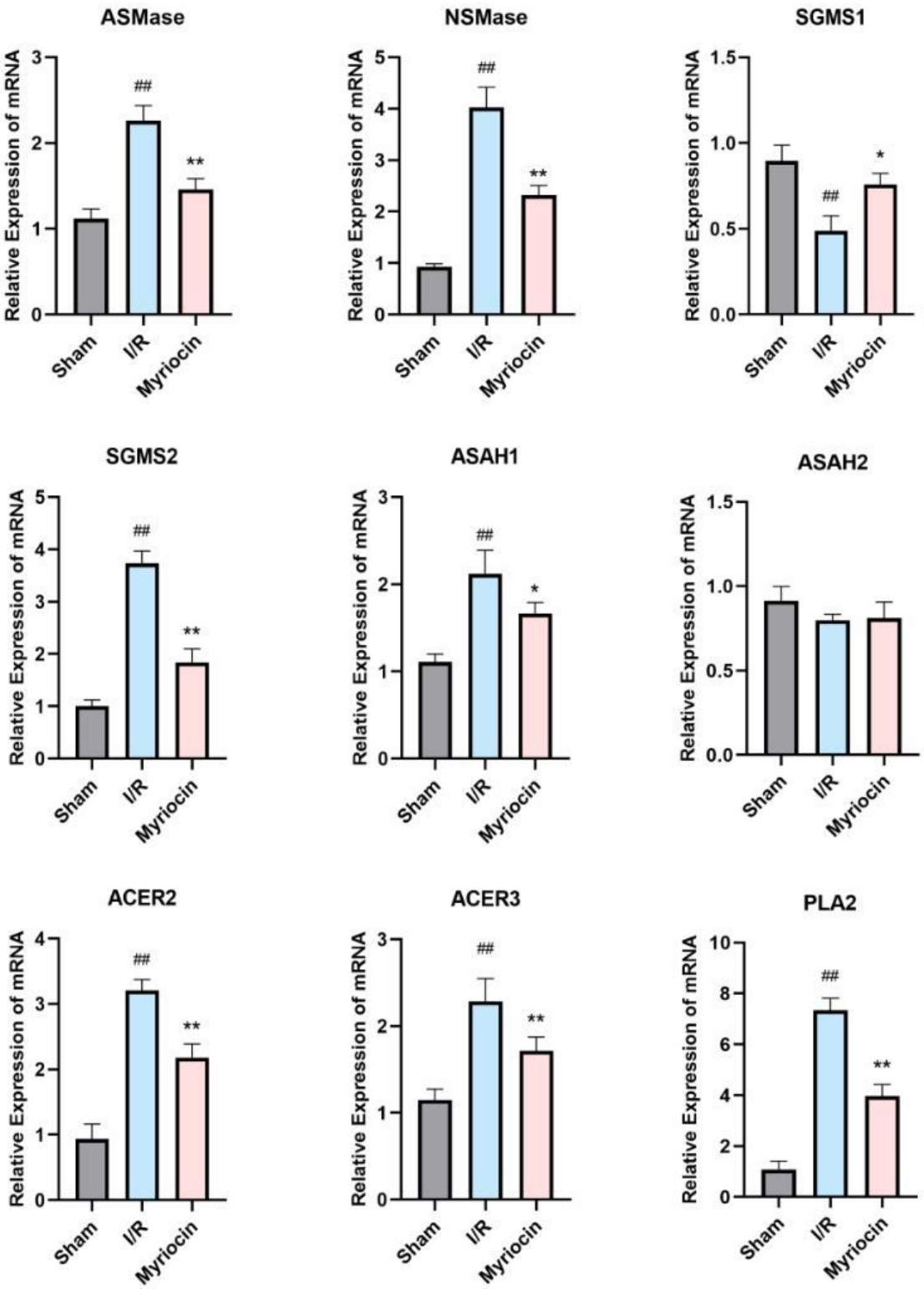

Figure 6

Myriocin influenced the expression levels of enzymes genes involved in the pathways of altered metabolites. RT-qPCR analysis of the enzymes gene involved in sphingolipid and glycerophosphospholipid metabolism of the cerebral cortical tissue of rats. Data are presented as mean ± SD (n=3). Compared with the Sham group, $^{\#\#}P < 0.01$; Compared with the I/R group $^{*}P < 0.05$, $^{**}P < 0.01$.

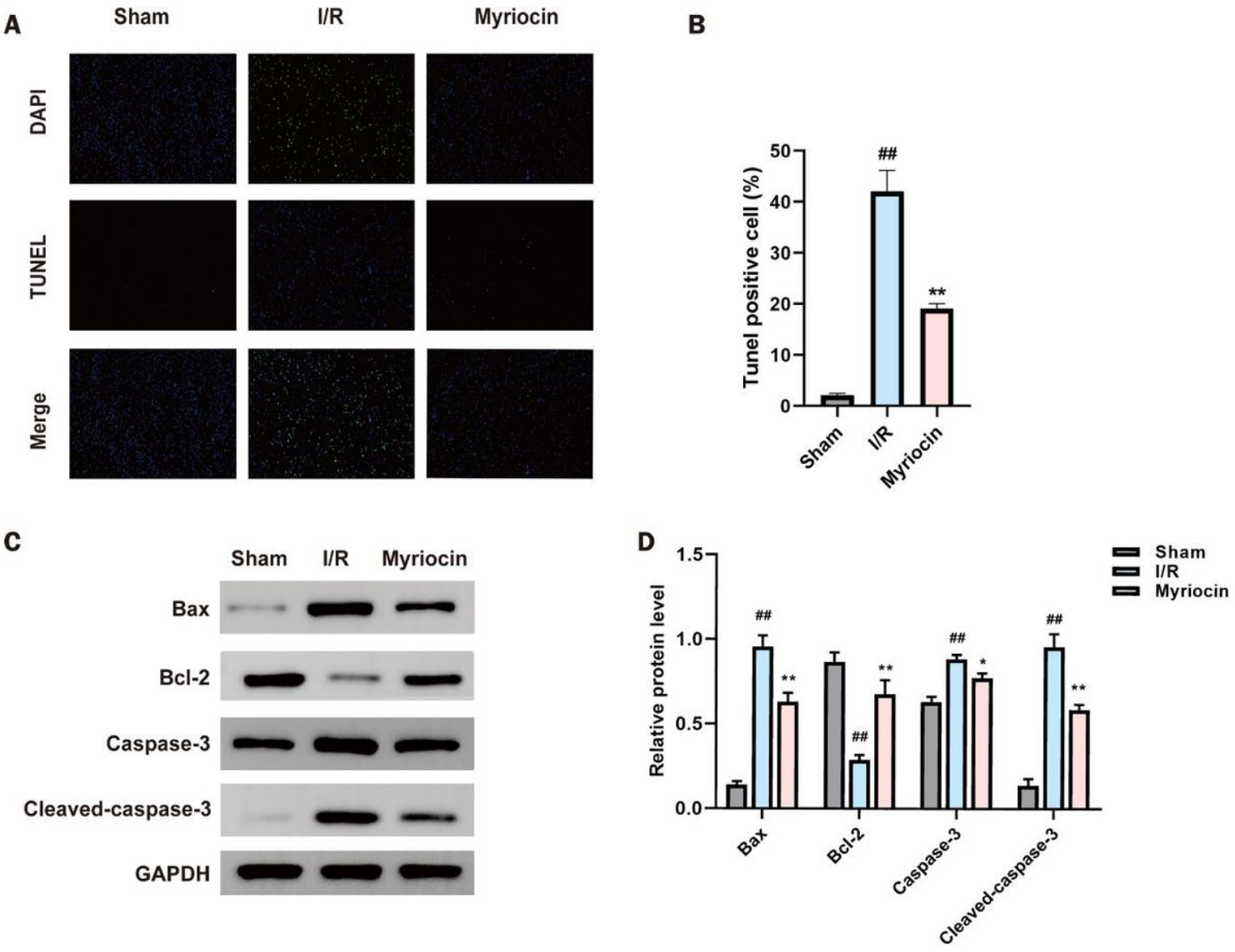

Figure 7

Myriocin inhibited relative apoptotic molecular expression levels. (A) Representative images of TUNEL staining of rat brain tissue. (B) The quantification of TUNEL positive cell in each group (magnification 200×, n=3). (C)The protein levels of Bax, Bcl-2, caspase-3 and cleaved caspase-3 were analyzed by western blot. (D) The quantification of relative protein in each group. Data are presented as mean ± SD (n=3). Compared with the Sham group, $^{\#\#}P < 0.01$; Compared with the I/R group $^{*}P < 0.05$, $^{**}P < 0.01$.

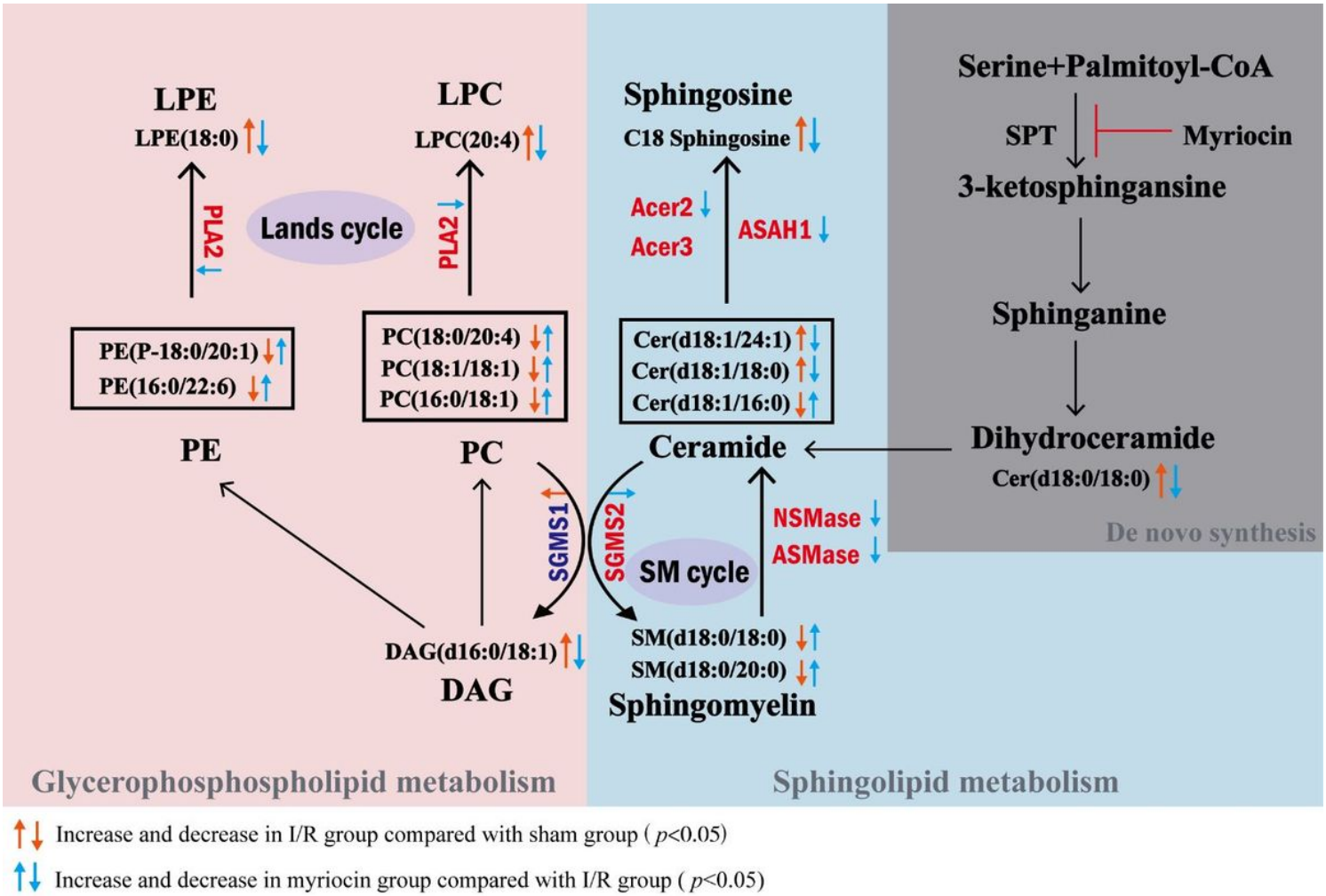

Figure 8

Disturbed lipid metabolic regulatory network in cerebral I/R model rats and the interventional effects of myriocin. The red and blue font represents the related enzymes were increased or decreased, respectively, in I/R group compared with sham group. The related enzymes reversed by myriocin are marked with up and down arrows.

Supplementary Files

This is a list of supplementary files associated with this preprint. Click to download.

- supplementarymaterial.docx